AN ANALYSIS OF TURBULENT BOUNDARY LAYER ALONG A FLAT PLATE

SHIGEO UCHIDA* and KIYOSHI MATSUMIYA**

Department of Aeronautical Engineering

(Received May 27, 1966)

A unified velocity distribution of turbulent incompressible boundary layer along a flat plate is calculated by assuming polynomials of the third degree for shearing stress and for mixing length. Introducing laminar sublayer it is found that the velocity distributions are well coincident with those of wall law and of velocity defect law in the region near wall and external boundary, respectively. In pure laminar flow it coincides with Kármán-Pohlhausen's profile. Solving the momentum integral equation by these velocity profiles a resistance formula is derived. This formula agrees well with Blasius'- and Prandtl-Schlichting's law in respective extremities of Reynolds number, while it gives poor results at transition region.

1. Introduction

The logarithmic law in turbulent boundary layers given by Prandtl[1] can be derived by the momentum transfer theory with assumed distributions of mixing length. Taking account of both laminar and turbulent shear stress this idea was extended to the turbulent flow with laminar sublayer. Refined formulae have been presented by Rotta,[2] Reichardt[3] and van Driest.[4]

Since the derivation has no difference for other configurations, *i.e.* for channel or pipe, these velocity distributions have been widely used as the universal law. This "wall law", however, does not satisfy the boundary conditions at the outer edge and, thereofre, it can not be applied to the whole section.

In the outer region of turbulent boundary layer a similarity rule called the "velocity defect law" was presented by von Kármán.[5] This is also a universal law with wide applications excepting the inner region very close to the wall.

These formulae have been verified with many experimental data, for instance, by Nikuradse,[6] Laufer[7] for a circular pipe, by Nikuradse,[8] Laufer[9] for a channel, and by Schultz-Grunow[10] and Klebanoff and Diehl[11] for a flat plate.

As it is shown by many experiments each curve of these formulae, which belongs to two different families, can not cover the whole section of turbulent boundary layer. The full profile has been presented by Reichardt[3] and Deissler[12] by introducing the turbulent viscosity coefficient, and Clauser[13] and Coles[14] have also presented a full profile by combining these two families.

In order to calculate the relation of shear stress or frictional drag to Reynolds number it is necessary to know the velocity distribution through whole section of boundary layer. In this connection Prandtl[1] assumed a shifted logarithmic

* Professor

** Graduate Student

distribution to satisfy the wall condition and calculated the resistance formula for a flat plate, which was transformed later into a functional form by Schlichting and has been verified its excellent result.

Basing on the very careful measurements on the flow along a flat plate Schultz-Grunow[10] found an empirical form of velocity distribution, which corrects the original logarithmic distribution of the velocity defect law, and obtained a resistance formula by using this distribution as the full profile.

Considering these situations it will be important to find a unified theory to derive the full profile of turbulent boundary layer. In this connection the present authors tried to have insight into the flow mechanism in the boundary layer and intended to develope a new expression of full profile, which enables us to calculate the resistance formula. The basic conception of Kârmân-Pohlhausen's method[15] in laminar boundary layer has been referred to the present work. In place of the polynomial expression of velocity profile we introduce the distributions of shearing stress and of mixing length both expressed by polynomials of the third order. Since these expressions satisfy the boundary conditions at the wall and at the outer edge, the derived full profile of velocity distribution satisfies the boundary conditions at both ends.

The relation between shearing stress and momentum thickness calculated from this profile is substituted into momentum integral equation to give the corresponding x-Reynolds number along a flat plate. The resistance formula is easily calculated by the use of the relation between shearing stress and this x-Reynolds number.

The major part of calculation can not be expressed into closed functional forms and numerical process has often be employed. The results are quite reasonable ones comparing with the existing informations.

2. Shearing Stress

The two-dimensional flow of incompressible fluid along a plate is concerned. Taking coordinate x along the plate and y normal to it, the flow is governed by the equations of motion for boundary layer:

$$\rho u\frac{\partial u}{\rho x}+\rho v\frac{\partial u}{\partial y}=-\frac{\partial p}{\partial x}+\frac{\partial \tau}{\partial y} \tag{1}$$

$$\frac{\partial p}{\partial y}=0, \tag{2}$$

where u, v are x, y components of the velocity, respectively. Density ρ has a constant value and pressure p is an only function of x.

Shearing stress τ has the following boundary vaues:

$$\tau=\tau_0 \quad \text{at} \quad y=0 \tag{3}$$

$$\tau=0 \quad \text{at} \quad y=\delta, \tag{4}$$

where δ denotes the thickness of boundary layer.

Two more boundary conditions are added by requesting Eq. (1) to be held along the wall and on the outer edge. Substitution of $u=v=0$ in Eq. (1) gives

$$\frac{\partial \tau}{\partial y} = \frac{dp}{dx} \quad \text{at} \quad y = 0. \tag{5}$$

The condition of smooth connection with the external flow of velocity u_e is expressed by $u = u_e$ and $\partial u/\partial y = 0$. These conditions transform Eq. (1) into the form:

$$\frac{\partial \tau}{\partial y} = \rho u_e \frac{du_e}{dx} + \frac{dp}{dx} \quad \text{at} \quad y = \delta, \tag{6}$$
$$= 0$$

where the condition of potential flow at the outer edge is applied.

The shearing stress is now assumed to be expressed by series expansion up to the third degree in order to satisfy the four conditions. Introducing a parameter of pressure gradient

$$P = \frac{\delta}{\tau_0} \frac{dp}{dx},$$

a polynomial expression of τ is given by using Eqs. (3)-(6):

$$\frac{\tau}{\tau_0} = 1 + P\eta - (3 + 2P)\eta^2 + (2 + P)\eta^3 \tag{7}$$

where $\eta = y/\delta$. For a flat plate it is simplified by putting $P = 0$:

$$\frac{\tau}{\tau_0} = 1 - 3\eta^2 + 2\eta^3 \tag{8}$$

This distribution of shearing stress is given in Fig. 1, where other curves show the component of turbulent shear stress which is calculated in the following chapters. Comparing with the measured distribution by Schultz-Grunow[10] as shown in Fig. 2, the present profile seems to be a reasonable one.

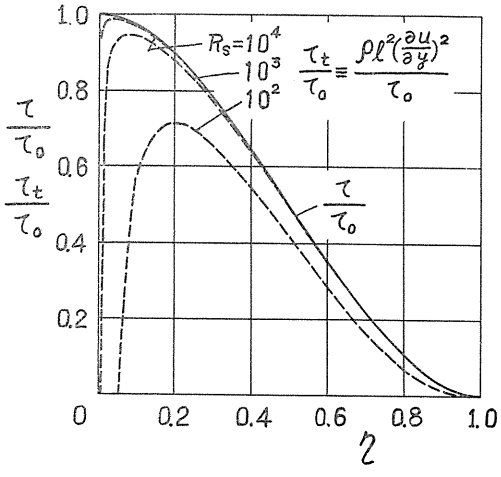

FIG. 1. Distribution of shearing stress.

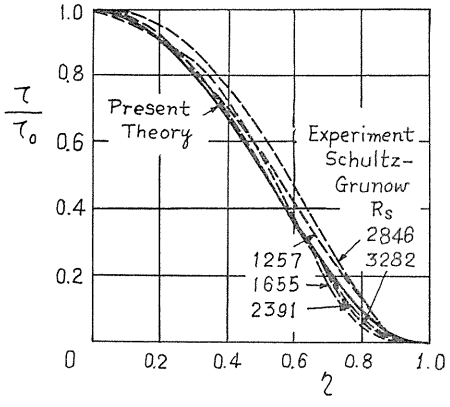

FIG. 2. Shearing stress.

3. Mixing Length

The laminar sublayer of thickness y_l is considered, where y_l is assumed to change following the empirical law:

$$v_* y_l/\nu = \text{constant} = A, \tag{9}$$

where $v_* = \sqrt{\tau_0/\rho}$ denotes the frictional velocity and ν the kinematic viscosity. In the following calculation $A=5$ is employed for the smooth flat plate.

According to Rotta's idea we assume that the mixing length is vanished in laminar sublayer and that it starts to grow up at the outer edge of sublayer. In this connection we can put the following boundary condition to the distribution of mixing length:

$$\left.\begin{aligned} &l=0,\ dl/dy=\kappa \quad \text{at} \quad y=y_l \\ &l=l_e,\ dl/dy=0 \quad \text{at} \quad y=\delta \end{aligned}\right\} \tag{10}$$

where l_e denotes an empirical value of mixing length at the outer edge. Some experiments[10] seem to show that the mixing length tends to a finite value close to the external region.

We assume now an expression in series expansion up to the third degree for the mixing length, where coefficients are determined by four boundary conditions of Eq. (10). Introducing a parameter $\lambda \equiv l_e/\delta$, it is given by

$$\begin{aligned} l/\delta &= \lambda + C_2(1-\eta)^2 + C_3(1-\eta)^3 \\ &= (\lambda + C_2 + C_3) - (2C_2 + 3C_3)\eta \\ &\qquad + (C_2 + 3C_3)\eta^2 - C_3\eta^3, \end{aligned} \tag{11}$$

where

$$C_2 = \frac{\kappa(1-\eta_l) - 3\lambda}{(1-\eta_l)^2}, \quad C_3 = -\frac{\kappa(1-\eta_l) - 2\lambda}{(1-\eta_l)^3}$$

and $\eta_l \equiv y_l/\delta = A/(v_*\delta/\nu)$.

A sectional Reynolds number is now introduced, defining

$$R_s = \frac{v_*\delta}{\nu}. \tag{12}$$

It will be easily seen that the mixing length is a function of parameters κ, λ, A and R_s. In the present calculation $\kappa=0.4$, $\lambda=0.06$ and $A=5$ are employed.

Comparing with the measurement by Schultz-Grunow[10] the present expression seems to be valid as shown in Fig. 3.

Assuming the law on laminar sublayer given by Eq. (9) to be formally effective over whole region of Reynolds number, the distributions of mixing length are calculated as shown in Fig. 4.

It is found that the flow becomes pure laminar for $R_s \leqq A(=5)$. The interpretation of flow mechanism in intermediate region of $5 < R_s < 100$ belongs to a future problem. The coexistence of laminar and turbulent layer with same order of thickness is a little doubtful phenomena, since it has not been confirmed in experiments.

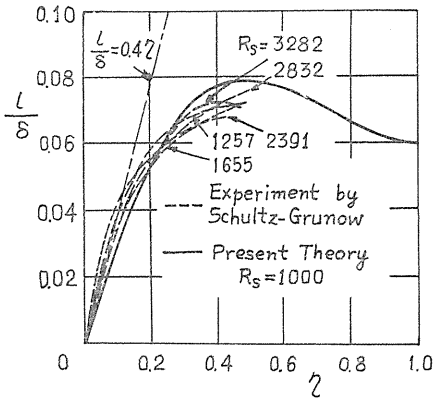

FIG. 3. Mixing length.

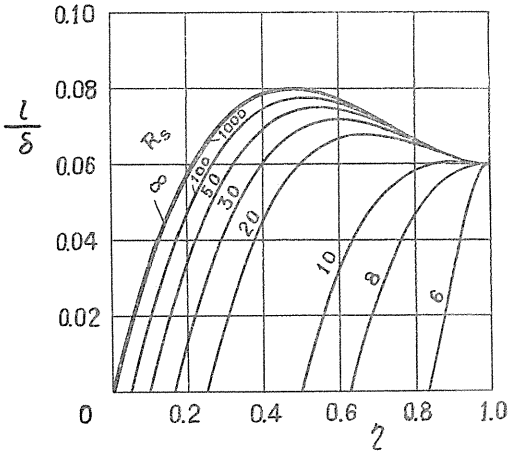

FIG. 4. Distribution of mixing length.

4. Velocity Distributions

Within a laminar sublayer the turbulent shears tress is assumed to be decayed off and, therefore, it is given

$$\tau = \mu \frac{\partial u}{\partial y}. \tag{13}$$

The non-dimensionalized velocity gradient is obtained by Eq. (13). Putting Eq. (8) we have

$$\frac{\partial(u/v_*)}{\partial(y/\delta)} = \frac{v_*\delta}{\nu}\frac{\tau}{\tau_0} = R_s(1-3\eta^2+2\eta^3) \tag{14}$$

Integration of Eq. (14) with the boundary condition, $u=0$ at $\eta=0$, gives the velocity distribution in laminar sublayer:

$$\frac{u}{v_*} = R_s\left(\eta-\eta^3+\frac{1}{2}\eta^4\right) \tag{15}$$

In the major part of turbulent boundary layer the shearing stress should be considered in more general form. The equation of motion for the mean velocity in a turbulent flow is reduced from Navier-Stokes' equation. With the boundary layer approximation it is given

$$\rho u\frac{\partial u}{\partial x}+\rho v\frac{\partial u}{\partial y} = -\frac{\partial p}{\partial x}+\frac{\partial}{\partial y}\left[\mu\frac{\partial u}{\partial y}-\rho\overline{u'v'}\right] \tag{16}$$

where u' and v' are velocity fluctuations in x and y direction, respectively. Comparing this equation with Eq. (1) the general expression for shearing stress is obtained as the sum of molecular shear and Reynolds stress.

$$\tau = \mu \frac{\partial u}{\partial y} - \rho \overline{u'v'} \tag{17}$$

It must be noticed that this expression of shearing stress is not a hypothetical one as that expressed by assuming the sum of laminar and turbulent shear stresses.

According to the conception of momentum transfer theory Eq. (17) is deformed.

$$\tau = \mu \frac{\partial u}{\partial y} + \rho l^2 \left(\frac{\partial u}{\partial y} \right)^2 \tag{18}$$

Eq. (18) is solved to give the velocity gradient

$$\frac{\partial u}{\partial y} = \sqrt{\frac{\tau}{\rho l^2} + \frac{\nu^2}{4l^4}} - \frac{\nu}{2l^2}.$$

It is non-dimensionalized as follows:

$$\frac{\partial (u/v_*)}{\partial (y/\delta)} = \sqrt{\frac{\tau/\tau_0}{(l/\delta)^2} + \frac{1}{4 R_s^2 (l/\delta)^4}} - \frac{1}{2 R_s (l/\delta)^2}. \tag{19}$$

Substituting Eqs. (8) and (11) with fixed value of $\kappa = 0.4$ and $\lambda = 0.06$ Eq. (19) can be integrated numerically to give the velocity distribution beyond $\eta \geqq \eta_l$, the initial value u_l at $\eta = \eta_l$ is supplied from Eq. (15):

$$u_l / v_* = R_s (\eta_l - \eta_l^3 + \eta_l^4/2) \tag{20}$$

At the edge of laminar sublayer the mixing length tends to zero and the velocity gradient in Eq. (19) has an expression $\infty - \infty$. This is easily shown to tend a finite value by the use of series expansion.

$$\frac{\partial (u/v_*)}{\partial (y/\delta)} = R_s \frac{\tau}{\tau_0} - R_s \left(R_s \frac{\tau}{\tau_0} \right)^2 \left(\frac{l}{\delta} \right)^2 + 2 R_s^2 \left(R_s \frac{\tau}{\tau_0} \right)^3 \left(\frac{l}{\delta} \right)^4 + \cdots \tag{21}$$

It can be integrated in the region close to the edge of sublayer:

$$\begin{aligned} u/v_* = {} & u_l/v_* + a_1 (\eta - \eta_l) + a_2 (\eta - \eta_l)^2 \\ & + (a_3 - R_s a_1^2 \kappa^2/3) (\eta - \eta_l)^3 \\ & + (a_4 - R_s a_1^2 \kappa k/2 - R_s a_1 a_2 \kappa^2) (\eta - \eta_l)^4 + \cdots \end{aligned} \tag{22}$$

where

$$a_1 = R_s (1 - 3\eta_l^2 + 2\eta_l^3),\ a_2 = -3 R_s \eta_l (1 - \eta_l),\ a_3 = -R_s (1 - 2\eta_l)$$
$$a_4 = R_s/2,\ k = -\{2\kappa (1 - \eta_l) - 3\lambda\}/(1 - \eta_l)^2$$

Eq. (22) was used as an auxiliary expression to check some part of integration.

As the velocity gradient approaches to the numerical value of R_s, which takes a very large value at high Reynolds number, in the wall region, each division for the numerical integration of Eq. (19) should be taken as small as the order of R_s^{-1} in the region close to the edge of sublayer.

The integration through full section;

$$\int_0^1 \frac{\partial(u/v_*)}{\partial(y/\delta)} d\eta = \frac{u_e}{v_*}, \tag{23}$$

gives an important factor u_e/v_*, which is directly connected with the local skin friction as shown in the following paragraph.

Dividing the velocity distribution u/v_* by u_e/v_*, we have the full sectional profile of velocity u/u_e as the function of y/δ. Numerical values are given in Table 1 (a), 1 (b) and in Fig. 5. It is easily seen that the profile for $R_s \leqq 5$ is coincident with Kârmân-Pohlhausen's laminar profile.

Comparing with experiments[10) 11)] the present velocity profile shows to be fairly good results as in Figs. 6 and 7, where Reichardt and others' experiments[16)]

TABLE 1 (a). Velocity Profile-1

η	R_s							
	5	10	20	30	50	100	200	500
0	0	0	0	0	0	0	0	0
.010								.2286
.015								.3231
.020								.3793
.025							.2623	
.040							.3862	
.050	.0998	.1003	.1127	.1339	.1813	.2995		
.060						.3563	.4728	.5524
.100	.1981	.1991	.2239	.2659	.3600	.4975	.5672	.6237
.200	.3856	.3876	.4358	.5145	.5970	.6548	.6899	.7246
.300	.5541	.5570	.6232					
.400	.6976	.7013	.7545	.7785	.7961	.8117	.8248	.8411
.500	.8125	.8168						
.600	.8976	.9012	.9099	.9113	.9114	.9124	.9153	.9213
.700	.9541							
.800	.9856	.9858	.9851	.9837	.9814	.9787	.9776	.9780
.900	.9981							
1	1	1	1	1	1	1	1	1

TABLE 1 (b). Velocity Profile-2

η	R_s								
	1×10	2×10	5×10	1×10	2×10	5×10	1×10	2×10	5×10
0	0	0	0	0	0	0	0	0	0
.00001									.1278
.00005							.1415	.2207	.2785
.0001						.1489	.2327		
.0005				.1689	.2625	.3343		.4081	.4378
.001			.1793	.2777	.3384	.3923	.4275	.4561	.4828
.002			.2948	.3581	.4027	.4471	.4781	.5053	.5275
.004		.2883							
.005	.2108								
.006	.2511	.3517	.4266	.4653	.4975	.5323	.5581	.5789	.5991
.010	.3497	.4182	.4780	.5112	.5398	.5712	.5949	.6137	.6322
.020	.4509	.4983	.5451	.5728	.5972	.6243	.6453	.6614	.6776
.060	.5899	.6199	.6527	.6730	.6914	.7119	.7284	.7403	.7526
.100	.6529	.6772	.7046	.7216	.7373	.7546	.7691	.7788	.7893
.200	.7443	.7615	.7813	.7938	.8055	.8181	.8294	.8360	.8438
.400	.8515	.8610	.8722	.8795	.8864	.8936	.8989	.9041	.9087
.600	.9259	.9303	.9358	.9394	.9429	.9465	.9491	.9518	.9541
.800	.9789	.9800	.9814	.9824	.9834	.9845	.9852	.9860	.9867
1	1	1	1	1	1	1	1	1	1

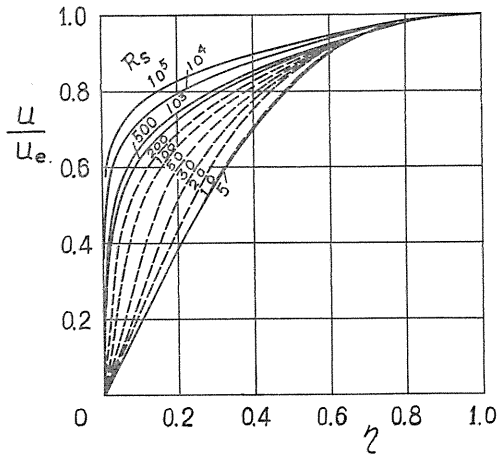

FIG. 5. Velocity distribution.

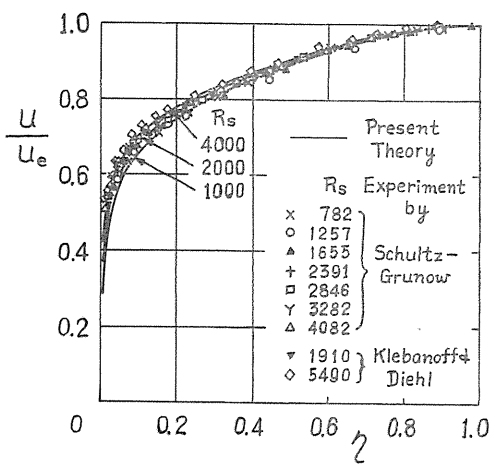

FIG. 6. Velocity distribution compared with experiments.

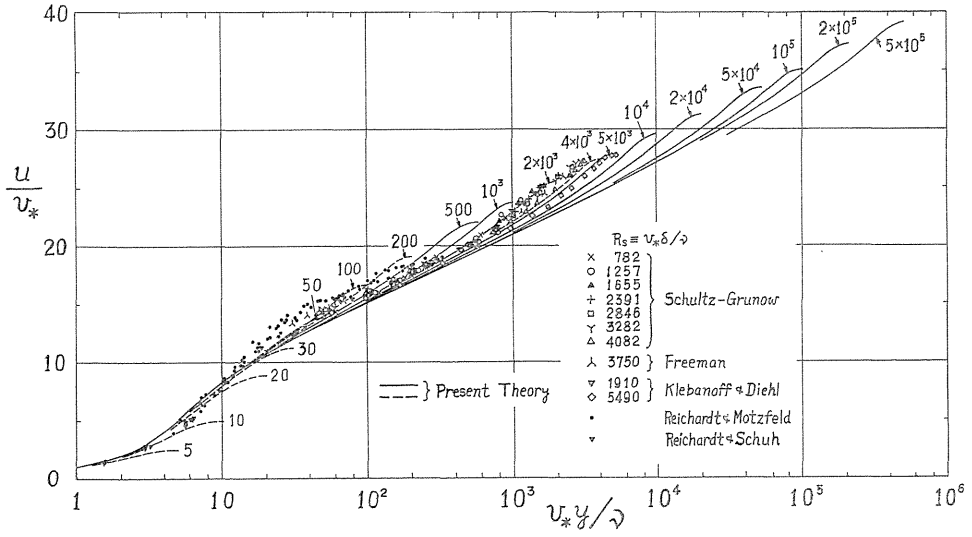

FIG. 7. Logarithmic expression of velocity distributions.

for a circular pipe are also added for the reference in order to show the velocity profile close to the wall. If it is noticed that the range of $R_s \geqq 10^3$ is corresponding to the range of $R_x \geqq 10^6$, we can see from Fig. 7 that the velocity distribution has a close relation with logarithmic law in the intermediate y-region of the boundary layer.

In order to examine the velocity distribution on the basis of the velocity defect law the decrement of velocity from the external velocity is calculated and is shown in Figs. 8 and 9 comparing with experiments. It is found that the present theory produces almost single relation between $(u_e - u)/v_*$ to y/δ in the

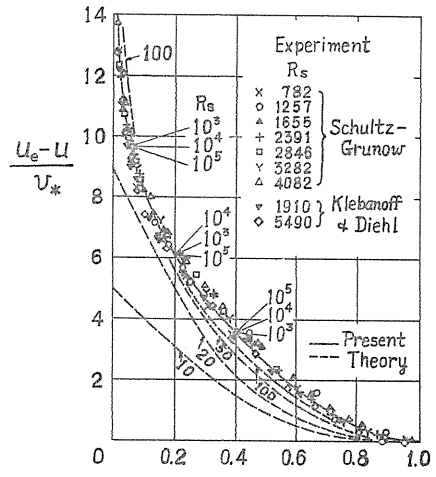

FIG. 8. Distribution in the velocity defect law.

range of $R_s \geqq 10^3$, while the other curves for $5 < R_s < 10^3$ might not be valid. These illustration seems to show the validity of the present calculation.

The behaviour of velocity distributions close to the outer edge can be calculated in the followings. Putting

$$\zeta = 1 - \eta$$

into Eqs. (8) and (11) we have

$$\tau/\tau_0 = 3\zeta^2 - 2\zeta^3, \tag{24}$$

$$l/\delta = \lambda + C_2\zeta^2 + C_3\zeta^3. \tag{25}$$

Eq. (19) can be deformed by Taylor expansion respecting ζ as follows:

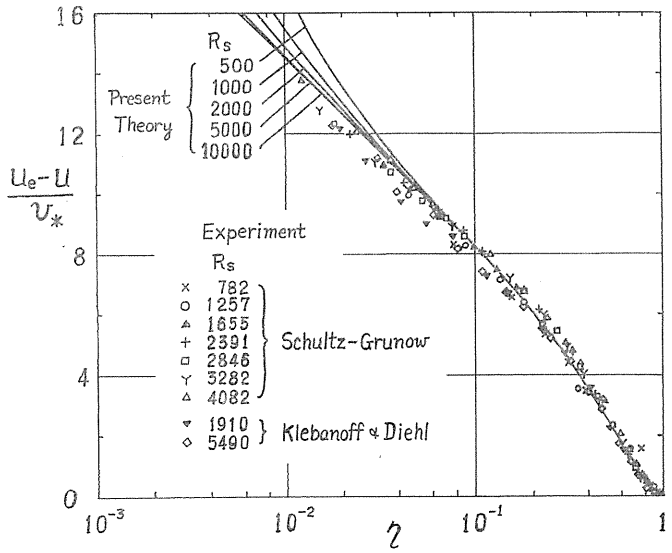

FIG. 9. Logarithmic expression of velocity defect law.

$$-\frac{\partial(u/v_*)}{\partial\zeta} = 3R_s\zeta^2 - 2R_s\zeta^3 - 9\lambda^2R_s^3\zeta^4 + 12\lambda^2R_s^3\zeta^5 + \cdots \tag{26}$$

Integration of Eq. (26) with the boundary condition

$$u = u_e \quad \text{at} \quad \zeta = 0 \tag{27}$$

gives

$$\frac{u_e - u}{v_*} = R_s\zeta^3 - \frac{1}{2}R_s\zeta^4 - \frac{9}{5}\lambda^2R_s^3\zeta^5 + 2\lambda^2R_s^3\zeta^6 + \cdots \tag{28}$$

It is easy to calculate the thickness of boundary layer by the use of velocity profile. The displacement thickness δ^* and the momentum thickness θ are calculated by the numerical integration of

$$\frac{\delta^*}{\delta} = \int_0^1 \left(1 - \frac{u}{u_e}\right) d\eta, \quad \frac{\theta}{\delta} = \int_0^1 \frac{u}{u_e}\left(1 - \frac{u}{u_e}\right) d\eta. \tag{29}$$

Obtained values are shown in Table 2 with those of u_e/v_*, $u_e\delta/\nu$, $u_e\delta^*/\nu$ and $u_e\theta/\nu$.

The non-monotonic change of θ/δ may be caused by the formal extension of the law of sublayer thickness, *i.e.* Eq. (9), into the intermediate region of small Reynolds numbers. The value $u_e\theta/\nu$ derived from θ/δ, however, shows a monotonic variation, since the change of R_s is much predominant.

TABLE 2. Parameters of Profile

R_s	$\frac{u_e}{v_*}$	$\frac{v_*}{u_e}$	$\frac{\delta^*}{\delta}$	$\frac{\theta}{\delta}$	$\frac{u_e\delta}{\nu}$	$\frac{u_e\delta^*}{\nu}$	$\frac{u_e\theta}{\nu}$	
1	0.500	2	.3000	.1175				A^*
2	1.000	1	.3000	.1175				
3	1.500	.6667	.3000	.1175				
4	2.000	.5000	.3000	.1175				
5	2.500	.4000	.3000	.1175	1.250×10	3.750	1.468	
10	4.974	.2011	.2979	.1167	4.974×10	1.482×10	5.806	
20	8.849	.1130	.2754	.1134	1.770×10^2	4.873×10	2.008×10	
30	11.17	.08949	.2545	.1129	3.352×10^2	8.531×10	3.784×10	
50	13.76	.07269	.2300	.1136	6.879×10^2	1.582×10^2	7.813×10	
1×10^2	16.65	.06005	.2042	.1144	1.665×10^3	3.400×10^2	1.904×10^2	
2×10^2	19.05	.05249	.1833	.1130	3.810×10^3	6.984×10^2	4.304×10^2	
5×10^2	21.87	.04573	.1621	.1088	1.093×10^4	1.773×10^3	1.190×10^3	
1×10^3	23.72	.04216	.1495	.1051	2.372×10^4	3.547×10^3	2.492×10^3	
2×10^3	25.52	.03919	.1391	.1013	5.103×10^4	7.097×10^3	5.171×10^3	
5×10^3	27.88	.03587	.1272	.09572	1.394×10^5	1.774×10^4	1.334×10^4	
1×10^4	29.60	.03379	.1199	.09203	2.960×10^5	3.549×10^4	2.724×10^4	
2×10^4	31.32	.03193	.1131	.08834	6.263×10^5	7.083×10^4	5.533×10^4	B^*
5×10^4	33.58	.02978	.1054	.08410	1.679×10^6	1.770×10^5	1.412×10^5	
1×10^5	35.32	.02831	.1001	.08049	3.532×10^6	3.536×10^5	2.843×10^5	
2×10^5	37.24	.02685	.0951	.07766	7.449×10^6	7.084×10^5	5.785×10^5	
5×10^5	39.11	.02557	.0906	.07459	1.955×10^7	1.771×10^5	1.458×10^6	

* Region A: pure laminar, B: fully turbulent.

5. Solution of the Momentum Integral Equation

The velocity profiles in individual section are obtained so far as functions of $R_s = v^*\delta/\nu$. In order to know the corresponding situation along x and to calculate the frictional drag coefficient as a function of Reynolds number, the momentum equation should be solved.

The momentum integral equation is given by

$$\frac{d\theta}{dx} + (2\theta + \delta^*)\frac{1}{u_e}\frac{du_e}{dx} = \frac{\tau_0/\rho}{u_e^2}. \tag{30}$$

For the flow along a flat plate it is simplified:

$$\frac{d\theta}{dx} = \left(\frac{v_*}{u_e}\right)^2. \tag{31}$$

It is noticed that v_*/u_e is available as a function of $u_e\theta/\nu$. Considering this condition Eq. (31) is deformed in the following expression:

$$\left(\frac{u_e}{v_*}\right)^2 d\left(\frac{u_e\theta}{\nu}\right) = d\left(\frac{u_e x}{\nu}\right). \tag{32}$$

Integration of Eq. (32) gives the relation between θ and x.

$$R_x \equiv \frac{u_e x}{\nu} = \int_0 \left(\frac{u_e}{v_*}\right)^2 d\left(\frac{u_e\theta}{\nu}\right), \tag{33}$$

where the integral constant is determined by the condition:

$$\theta = 0 \quad \text{at} \quad x = 0 \tag{34}$$

In the region of small Reynolds number, where $R_s \leqq 5$, the whole field is covered by laminar layer and, therefore, Eq. (15) can be applied to the whole section. Putting $\eta = 1$ into Eq. (15) we have

$$u_e/v_* = R_s/2 \tag{35}$$

The corresponding velocity profile

$$u/u_e = 2\eta - 2\eta^3 + \eta^4, \tag{36}$$

is found to be coincident with that given by Kârmân-Pohlhausen's theory. The momentum thickness can easily be calculated.

$$\theta/\delta = 37/315 \tag{37}$$

Combining Eqs. (35) and (37) we have

$$\left(\frac{u_e}{v_*}\right)^2 = \frac{1}{2}\frac{u_e\delta}{\nu} = \frac{315}{74}\frac{u_e\theta}{\nu} \tag{38}$$

By the use of this expression Eq. (32) can easily be integrated in an analytical form. Determining the integral constant by Eq. (34) we have

$$\frac{u_e x}{\nu} = \frac{315}{148}\left(\frac{u_e\theta}{\nu}\right)^2 \tag{39}$$

or

$$\frac{u_e\theta}{\nu} = \sqrt{\frac{148}{315}}\left(\frac{u_e x}{\nu}\right)^{1/2}. \tag{40}$$

At the edge of pure laminar region of the present theory, where $R_s = 5$, $u_e\theta/\nu$ and $u_e x/\nu$ have values of

$$\left(\frac{u_e\theta}{\nu}\right)_{R_s=5} = \frac{185}{126}, \quad \left(\frac{u_e x}{\nu}\right)_{R_s=5} = \frac{23125}{5040} \tag{41}$$

In order to calculate Eq. (33) beyond the region of $R_s \geqq 5$ the relation between $(u_e/v_*)^2$ and $u_e\theta/\nu$ is delivered from the previous result given in Table 2. It is

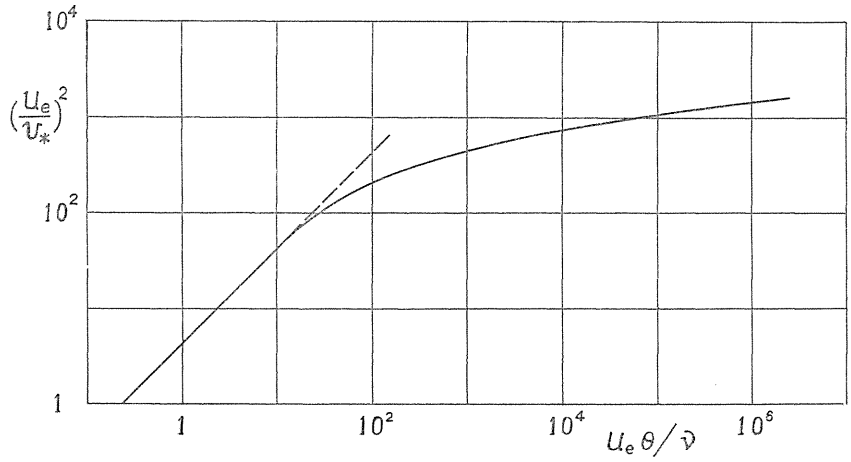

FIG. 10. Relation of $(u_e/v_*)^2$ to $u_e\theta/\nu$.

TABLE 3. Relation of R_x to $u_e\theta/\nu$

$\frac{u_e\theta}{\nu}$	$\left(\frac{u_e}{v_*}\right)^2$	$\frac{u_e x}{\nu}$	c'_f
1.46825	6.25	4.59	.320
2	8.52	8.52	.235
4	17.0	3.41×10	.118
6	25.5	7.66	.0784
8	34.0	1.36×10^2	.0588
1×10	42.3	2.13	.0473
2	78.0	8.21	.0256
4	129	2.93×10^3	.0155
6	164	5.87	.0122
8	190	9.41	.0105
1×10^2	212	1.34×10^4	.00946
2	282	3.85	.00709
4	356	1.03×10^5	.00562
6	400	1.79	.00500
8	432	2.62	.00463
1×10^3	457	3.51	.00438
2	536	8 51	.00373
4	619	2.01×10^6	.00323
6	670	3.31	.00299
8	708	4.69	.00283
1×10^4	738	6.13	.00271
2	829	1.40×10^7	.00241
4	930	3.17	.00215
6	992	5.09	.00202
8	1037	7.13	.00193
1×10^5	1072	9.24	.00187
2	1186	2.06×10^8	.00170
4	1308	4.57	.00153
6	1381	7.26	.00145
8	1432	1.01×10^9	.00140
1×10^6	1471	1.30	.00136

shown in Fig. 10. Using the interpolated values the integration in Eq. (33) is calculated as shown in Table 3.

For the practical use it is more convenient to express every quantity as a function of x-Reynolds number, *i.e.* $R_x\equiv u_e x/\nu$. Interpolating values in Table 3 such an expression is given in Table 4 and in Fig. 11. It is seen that all curves tend to Kármán-Pohlhausen's theory in pure laminar region, while that they approach closely turbulent law in the high Reynolds number region. In the region of $10^6\leqq R_x\leqq10^8$ we have approximately

$$u_e\delta/\nu = 0.100(u_e x/\nu)^{0.889} \quad (42)$$

$$u_e\delta^*/\nu = 0.046(u_e x/\nu)^{0.809} \quad (43)$$

$$u_e\theta/\nu = 0.019(u_e x/\nu)^{0.846} \quad (44)$$

$u_e\delta^*/\nu$ is very close to the value obtained from the 1/7-th power velocity distribution law, which is written.

$$u_e\delta^*/\nu = 0.046(u_e x/\nu)^{4/5} \quad (45)$$

TABLE 4. Variation of Parameters with R_x

R_x	R_s	$\frac{\delta^*}{\delta}$	$\frac{\theta}{\delta}$	$\frac{u_e\delta}{\nu}$	$\frac{u_e\delta^*}{\nu}$	$\frac{u_e\theta}{\nu}$
4.588	5.00	.300	.1175	1.25×10	3.75	1.468
6	5.37	.300	.1175	1.44	4.32	1.69
8	5.74	.300	.1174	1.65	4.95	1.94
1×10	6.10	.300	.1174	1.85	5.55	2.17
2	7.27	.300	.1174	2.61	7.82	3.06
4	8.63	.299	.1171	3.71	1.11×10	4.34
6	9.40	.298	.1169	4.38	1.31	5.12
8	1.30×10	.297	.1166	5.26	1.56	6.14
1×10^2	1.09	.297	.1164	5.90	1.75	6.87
2	1.32	.293	.1155	8.42	2.46	9.72
4	1.60	.286	.1144	1.21×10^2	3.45	1.38×10
6	1.81	.280	.1138	1.49	4.17	1.70
8	1.98	.276	.1135	1.74	4.80	1.97
1×10^3	2.13	.273	.1133	1.96	5.34	2.22
2	2.71	.260	.1129	2.86	7.43	3.23
4	3.53	.246	.1129	4.23	1.04×10^2	4.78
6	4.15	.238	.1132	5.35	1.28	6.06
8	4.71	.233	.1134	6.36	1.48	7.22
1×10^4	5.23	.228	.1136	7.30	1.67	8.30
2	7.36	.215	.1142	1.14×10^3	2.45	1.30×10^2
4	1.07×10^2	.202	.1143	1.79	3.62	2.05
6	1.35	.195	.1140	2.39	4.65	2.72
8	1.62	.189	.1136	2.95	5.58	3.35
1×10^5	1.84×10^2	.187	.1132	3.46×10^3	$6\,46\times10^2$	3.92×10^2
2	2.88	.174	.1115	5.84	1.20×10^3	6.51
4	4.71	.164	.1092	1.02×10^4	1.66	1.11×10^3
6	6.27	.158	.1077	1.41	2.23	1.52
8	7.79	.154	.1065	1.78	2.74	1.90
1×10^6	9.23	.151	.1056	2.16	3.27	2.28
2	1.57×10^3	.143	.1024	3.89	5.56	3.98
4	2.69	.135	.0993	7.06	9.55	7.01
6	3.73	.131	.0974	1.01×10^5	1.32×10^4	9.80
8	4.71	.128	.0961	1.30	1.66	1.25×10^4
1×10^7	5.60	.126	.0952	1.58	1.99	1.50
2	9.87	.120	.0921	2.93	3.52	2.70
4	1.77×10^4	.114	.0891	5.50	6.28	4.90
6	2.49	.111	.0874	7.93	8.81	6.93
8	3.16	.109	.0862	1.03×10^6	1.12×10^5	8.84
1×10^8	3.83	.108	.0852	1.26	1.36	1.07×10^5
2	6.88	.103	.0823	2.38	2.45	1.96
4	1.25×10^5	.0983	.0795	4.50	4.42	3.58
6	1.78	.0959	.0781	6.48	6.22	5.06
8	2.27	.0944	.0772	8.47	8.00	6.54
1×10^9	2.74	.0934	.0766	1.03×10^7	9.66	7.92
2	5.00	.0906	.0726	2.01	1.82×10^6	1.46×10^6

6. Resistance Formula

The coefficient of local skin friction denoted by C'_f is easily calculated by

$$C'_f \equiv \frac{\tau_0}{(1/2)\,\rho u_e^2} = 2\left(\frac{v_*}{u_e}\right)^2 \tag{46}$$

The formulae in pure laminar region is obtained from Eqs. (38) and (40).

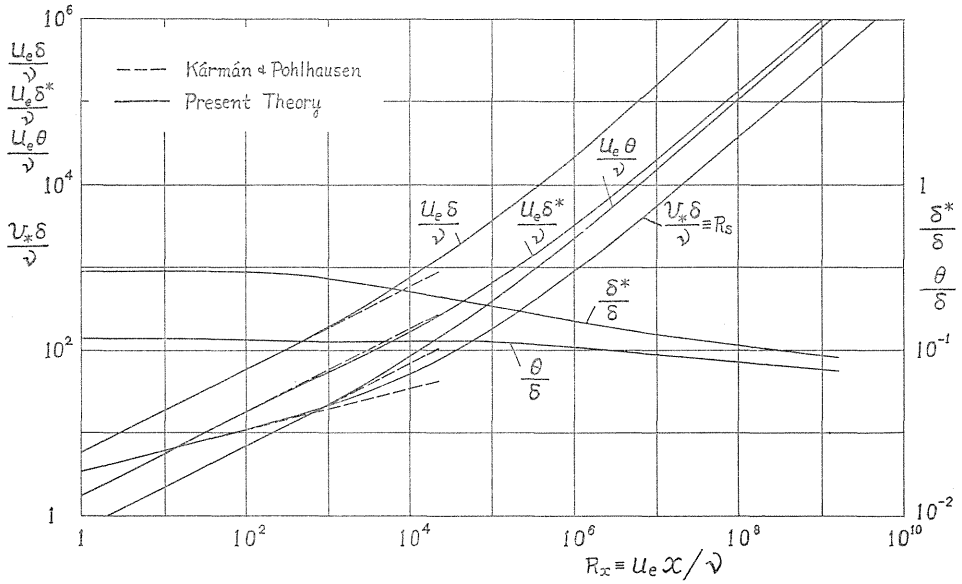

FIG. 11. Distributions of doundary layer thicknesses.

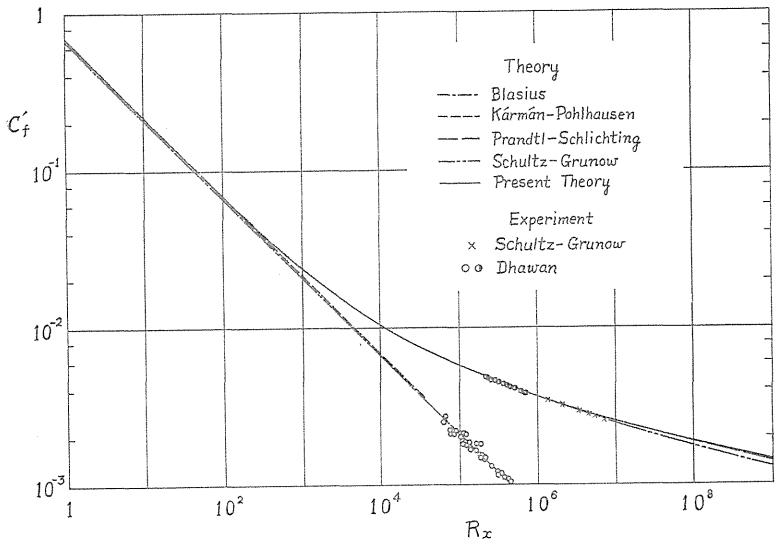

FIG. 12. The coefficient of local skin friction.

$$C_f' = \sqrt{148/315}\, R_x^{-1/2} \tag{47}$$

Numerical values of C_f' beyond $R_s \geqq 5$ is given in Tables 3 and 5 and is shown in Fig. 12. Comparing with theories by Prandtl-Schlichting[1] and Schultz-Grunow[10] and with experiments by Schultz-Grunow[10] and Dhawan,[17] C_f' of the present

TABLE 5. Coefficients of Skin Friction

R_x	c'_f	c_f	R_x	c'_f	c_f
4.588	.320	.640	1×10^5	.00568	.00785
6	.280	.560	2	.00492	.00654
8	.242	.485	4	.00426	.00554
1×10	.217	.434	6	.00396	.00506
2	.154	.307	8	.00376	.00476
4	.109	.217	1×10^6	.00362	.00454
6	.0886	.177	2	.00324	.00398
8	.0767	.154	4	.00289	.00351
1×10^2	.0684	.137	6	.00272	.00327
2	.0484	.0971	8	.00261	.00312
4	.0351	.0688	1×10^7	.00252	.00301
6	.0293	.0565	2	.00229	.00270
8	.0258	.0492	4	.00208	.00244
1×10^3	.0235	.0443	6	.00197	.00230
2	.0178	.0322	8	.00190	.00221
4	.0139	.0239	1×10^8	.00185	.00214
6	.0121	.0202	2	.00169	.00195
8	.0111	.0181	4	.00155	.00178
1×10^4	.0103	.0166	6	.00148	.00169
2	.00844	.0129	8	.00144	.00163
4	.00703	.0103	1×10^9	.00141	.00159
6	.00640	.00908	2	.00131	.00147
8	.00598	.00835			

theory is found to be a reasonable one. In the high Reynolds number region it is almost identical with Prandtl-Schlichting's theory.

The coefficient of total skin friction which is denoted by c_f is calculated by the integration of c'_f along x.

$$c_f = \frac{1}{x}\int_0^x c'_f dx = \frac{1}{R_x}\int_0^{R_x} c'_f dR_x \qquad (48)$$

In pure laminar region we have

$$c_f = 2\sqrt{\frac{148}{315}}R_x^{-1/2} = 1.371\,R_x^{-1/2}, \qquad (49)$$

which is identical with Kármán-Pohlhausen's theory,[14] while the exact formula by Blasius is given by

$$c_f = 1.3282\,R_x^{-1/2} \qquad (50)$$

The integration of Eq. (48) beyond this region is performed again by the numerical method and we have the results as shown in Table 5 and in Figs. 13 and 14.

As shown in Fig. 13 the present theory gives a reasonable resistance formula in fully turbulent region. It is a little higher than Schultz-Grunow's theory[10] in $10^5 \leqq R_x \leqq 10^7$ and is almost identical with Prandtl-Schlichting's theory[1] in $10^7 \leqq R_x \leqq 10^9$.

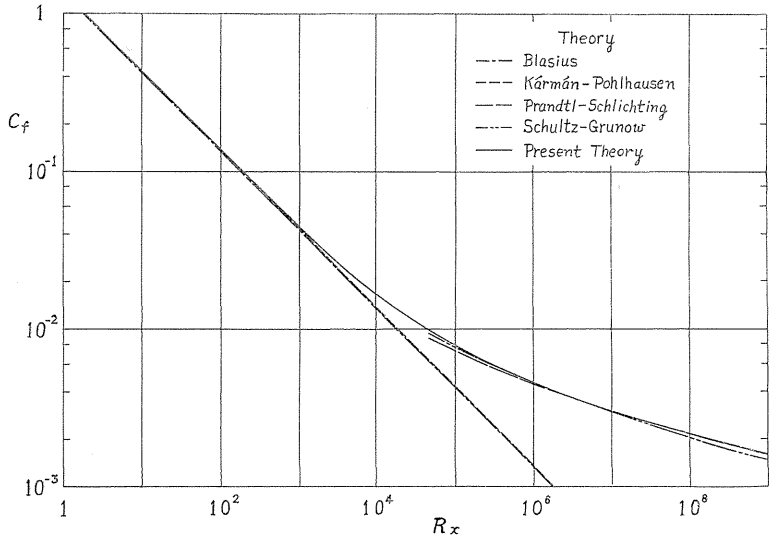

FIG. 13. The coefficient of total skin friction.

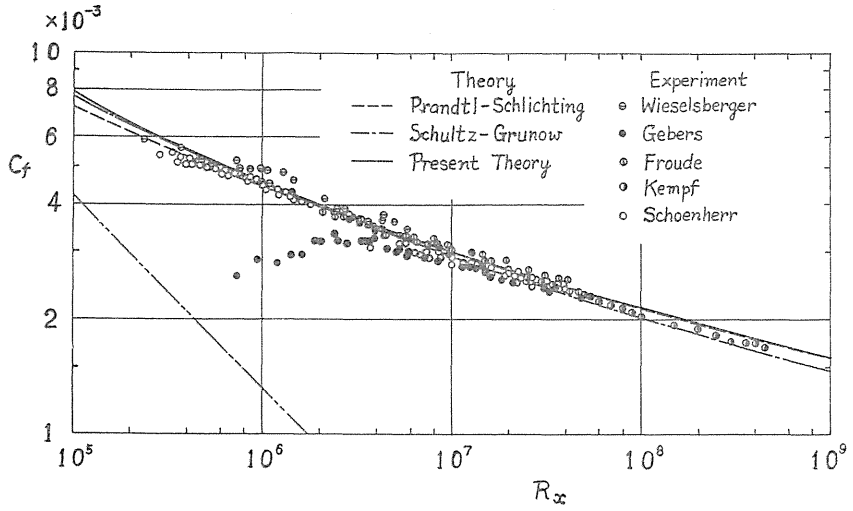

FIG. 14. The resistance formulae compared with experiments.

Starting from the pure laminar flow, which is identical with Kármán-Pohlhausen's theory,[15] c_f of the present calculation deviates gradually from the laminar law and connects smoothly with c_f in the fully turbulent region. The range of validity of the present theory may depend on the range of validity of the sublayer thickness law, which might not be effective in the intermediate range of R_x. It is well known that pure laminar flow can be maintained up to the order of $R_x=5\times10^5$, and the gradual shift from laminar to turbulent flow has not been observed. Whether it can be real under the special conditions or not, is not clear now and, therefore, precise investigations of flow mechanism in the intermediate range of R_x should be performed, as well as in the range of transition.

For the convenience of practical use a formula fit to the present calculation is derived in the same manner as Schlichting did.

$$c_f = 0.554(\log R_x)^{-2.68} \tag{51}$$

It is effective in the range of

$$5\times10^5 < R_x < 5\times10^8$$

The corresponding expression of Prandtl-Schlichting's formula is given as a reference.

$$c_f = 0.455(\log R_x)^{-2.58} \tag{52}$$

7. Conclusion

A unified method to calculate the turbulent flow along a flat plate is investigated. Assuming polynomial expressions for shearing stress and mixing length a reasonable form of velocity profile and corresponding coefficients of skin friction

are obtained as functions of x-Reynolds number. Whole things seem to be reduced and explained by a few parameter contained in the mixing length, *i.e.* κ and λ, and by the law on the thickness of laminar sublayer, *i.e.* $v_* y_l/\nu = \text{constant}$. In the present paper the latter is assumed to be extensible into a non fully developed turbulent flow. The results in this intermediate R_x region may only be a formal one.

In fully developed turbulent region, however, the present velocity profile and the calculated resistance formula are found to be quite reasonable ones.

References

1) L. Prandtl: Zur turbulenten Strömung in Rohren und längs Platten, Erg. Aerodyn. Vers.-Anst. zu Göttingen, IV Lief., München 1932, Oldenbourg, P. 18-29.
2) J. Rotta: Das in Wandnähe gültige Geschwindigkeitsgesetz turbulenter Strömungen, Ing.-Arch. **18**, P. 277-280 (1950).
3) H. Reichardt: Vollständige Darstellung der turbulenten Geschwindigkeitsverteilung in glatten Leitungen, ZAMM **31**, P. 208-219 (1951).
4) E. R. van Driest: On turbulent flow near a wall, J. Aero. Sci. **23**, P. 1007-1011 (1956).
5) Th. von Kármán: Mechanische Ähnlichkeit und Turbulenz, Verhand. d. 3 Int. Kong. f. Tech. Mech., Stockholm 1931, Norstedt u. Söner, P. 85-93.
6) J. Nikuradse: Gesetzmäßigkeit der turbulenten Strömung in glatten rohren, VDI-Forschungsheft 356 (1932).
7) J. Laufer: The structure of turbulence in fully developed pipe flow, NACA TR 1174 (1954).
8) J. Nikuradse: Untersuchungen über die Geschwindigkeitsverteilung in turbulenten Strömungen, VDI-Forschungsheft 281 (1926).
9) J. Laufer: Investigation of turbulent flow in a twodimmensional channel, NACA TN 2124 (1950).
10) F. Schultz-Grunow: Neues Reibungswiderstandsgesetz für glatte Platten, Luftfahrtforschung **17**, P. 239-246 (1940).
11) P. S. Klebanoff and Z. W. Diehl: Some features of artificially thickened fully developed turbulent boundary layers with zero pressure gradient, NACA TN 2475 (1951).
12) R. G. Deissler: Analysis of turbulent heat transfer, mass transfer and friction in smooth tubes at high Prandtl and Schmidt numbers, NACA TN 3145 (1954).
13) F. H. Clauser: The turbulent boundary layer, Advances in App. Mech., IV, New York 1956, Academic Press, P. 1-51.
14) D. Coles: The problem of the turbulent boundary layer, ZAMP **5**, P. 181-203 (1954).
15) K. Pohlhausen: Zur näherungsweisen Integration der Differentialgleichung der laminaren Reibungsschicht, ZAMM **1**, P. 252-268 (1921).
16) H. Reichardt: Die Wärmeübertragung in turbulenten Reibungsschichten, ZAMM **20**, P. 297-328 (1940).
17) S. Dhawan: Direct measurements of skin friction, 1121 (1953).

APPENDIX. Velocity Distributions

$R_s=5$				$R_s=10$			
$\frac{y}{\delta}$	$\frac{l}{\delta}$	$\frac{u}{v_*}$	$\frac{u}{u_e}$	$\frac{y}{\delta}$	$\frac{l}{\delta}$	$\frac{u}{v_*}$	$\frac{u}{u_e}$
0		0	0	0		0	0
.1		.495	.1981	.1		.991	.1991
.2		.964	.3856	.2		1.928	.3876
.3		1.385	.5541	.3		2.771	.5570
.4		1.744	.6976	.4		3.488	.7013
.5		2.031	.8125				
.6		2.244	.8976	.5	0	4.063	.8168
.7		2.385	.9541	.55	.01788	4.293	.8631
.8		2.464	.9856	.6	.03184	4.482	.9012
.9		2.495	.9981	.8	.05808	4.903	.9858
1	0	2.500	1	1	.06000	4.974	1

$R_s=20$				$R_s=30$			
$\frac{y}{\delta}$	$\frac{l}{\delta}$	$\frac{u}{v_*}$	$\frac{u}{u_e}$	$\frac{y}{\delta}$	$\frac{l}{\delta}$	$\frac{u}{v_*}$	$\frac{u}{u_e}$
0		0	0	0		0	0
.1		1.981	.2239	.16	0	4.87	.4361
.2		3.856	.4358	.2	.01257	5.75	.5145
.25	0	4.727	.5341				
.3	.01819	5.514	.6232				
.4	.04464	6.677	.7545	.4	.05986	8.70	.7785
.6	.06683	8.052	.9099	.6	.07173	10.18	.9113
.8	.06512	8.717	.9851	.8	.06588	10.99	.9837
1	.06000	8.849	1	1	.06000	11.17	1

$R_s=50$				$R_s=100$			
$\frac{y}{\delta}$	$\frac{l}{\delta}$	$\frac{u}{v_*}$	$\frac{u}{u_e}$	$\frac{y}{\delta}$	$\frac{l}{\delta}$	$\frac{u}{v_*}$	$\frac{u}{u_e}$
0		0	0	0		0	0
				.05	0	4.99	.2995
.1	0	4.95	.3600	.06	.003936	5.93	.3563
.15	.01837	6.96	.5059	.1	.01843	8.24	.4975
.2	.03366	8.21	.5970	.2	.04656	10.91	.6548
.4	.06889	10.95	.7961	.4	.07428	13.52	.8117
.6	.07449	12.54	.9114	.6	.07605	15.19	.9124
.8	.06626	13.50	.9814	.8	.06644	16.30	.9787
1	.06000	13.76	1	1	.06000	16.65	1

$R_s=2\times10^2$				$R_s=5\times10^2$			
$\frac{y}{\delta}$	$\frac{l}{\delta}$	$\frac{u}{v_*}$	$\frac{u}{u_e}$	$\frac{y}{\delta}$	$\frac{l}{\delta}$	$\frac{u}{v_*}$	$\frac{u}{u_e}$
0		0	0	0		0	0
				.01	0	5.00	.2286
.025	0	5.00	.2623	.0125	.0009961	6.17	.2820
.0325	.002965	6.36	.3340	.015	.001984	7.07	.3231
.04	.005859	7.36	.3862	.02	.003938	8.29	.3793
.06	.01324	9.01	.4728	.06	.01847	12.08	.5524
.1	.02657	10.81	.5672	.1	.03115	13.64	.6237
.2	.05223	13.14	.6899	.2	.05541	15.85	.7246
.4	.07660	15.71	.8248	.4	.07790	18.39	.8411
.6	.07670	17.44	.9153	.6	.07706	20.15	.9213
.8	.06651	18.62	.9776	.8	.06654	21.39	.9780
1	.06000	19.05	1	1	.06000	21.87	1

$R_s=1\times10^3$				$R_s=2\times10^3$			
$\frac{y}{\delta}$	$\frac{l}{\delta}$	$\frac{u}{v_*}$	$\frac{u}{u_e}$	$\frac{y}{\delta}$	$\frac{l}{\delta}$	$\frac{u}{v_*}$	$\frac{u}{u_e}$
0		0	0	0		0	0
				.0025	0	5.00	.1960
				.00325	.0002997	6.37	.2496
.005	0	5.00	.2108	.004	.0005986	7.36	.2883
.006	.0003994	5.95	.2511	.006	.001392	8.97	.3517
.01	.001984	8.29	.3497	.01	.002965	10.67	.4182
.02	.005861	10.69	.4509	.02	.006811	12.71	.4983
.06	.02016	13.99	.5899	.06	.02100	15.82	.6199
.1	.03263	15.48	.6529	.1	.03336	17.28	.6772
.2	.05643	17.65	.7443	.2	.05694	19.43	.7615
.4	.07831	20.19	.8515	.4	.07852	21.97	.8610
.6	.07717	21.96	.9259	.6	.07723	23.74	.9303
.8	.06655	23.22	.9789	.8	.06656	25.00	.9800
1	.06000	23.72	1	1	.06000	25.52	1

$R_s=4\times10^3$				$R_s=5\times10^3$			
$\frac{y}{\delta}$	$\frac{l}{\delta}$	$\frac{u}{v_*}$	$\frac{u}{u_e}$	$\frac{y}{\delta}$	$\frac{l}{\delta}$	$\frac{u}{v_*}$	$\frac{u}{u_e}$
0		0	0	0		0	0
.00125	0	5.00	.1825	.001	0	5.00	.1793
.002	.0002997	7.34	.2679	.002	.0003994	8.22	.2948
.006	.001886	11.33	.4134	.006	.001985	11.90	.4266
.01	.003453	12.79	.4670	.01	.003550	13.33	.4780
.02	.007284	14.69	.5364	.02	.007378	15.20	.5451
.06	.02142	17.71	.6464	.06	.02150	18.20	.6527
.1	.03372	19.16	.6993	.1	.03379	19.64	.7046
.2	.05719	21.30	.7775	.2	.05724	21.78	.7813
.4	.07862	23.84	.8701	.4	.07864	24.32	.8722
.6	.07725	25.61	.9348	.6	.07726	26.09	.9358
.8	.06656	26.88	.9811	.8	.06656	27.36	.9814
1	.06000	27.40	1	1	.06000	27.88	1

$R_s = 1\times10^4$				$R_s = 2\times10^4$			
$\frac{y}{\delta}$	$\frac{l}{\delta}$	$\frac{u}{v_*}$	$\frac{u}{u_e}$	$\frac{y}{\delta}$	$\frac{l}{\delta}$	$\frac{u}{v_*}$	$\frac{u}{u_e}$
0		0	0	0		0	0
				.00025	0	5.00	.1597
.0005	0	5.00	.1689	.0005	.00009996	8.22	.2625
.001	.0001998	8.22	.2777	.001	.0002997	10.60	.3384
.002	.0005986	10.60	.3581	.002	.0006981	12.61	.4027
.006	.002181	13.77	.4653	.006	.002280	15.58	.4975
.01	.003744	15.13	.5112	.01	.003841	16.90	.5398
.02	.007566	16.95	.5728	.02	.007660	18.70	.5972
.06	.02166	19.92	.6730	.06	.02175	21.65	.6914
.1	.03394	21.36	.7216	.1	.03401	23.09	.7373
.2	.05734	23.49	.7938	.2	.05739	25.22	.8055
.4	.07868	26.03	.8795	.4	.07870	27.76	.8864
.6	.07727	27.80	.9394	.6	.07927	29.53	.9429
.8	.06656	29.08	.9824	.8	.06656	30.80	.9834
1	.06000	29.60	1	1	.06000	31.32	1

$R_s = 5\times10^4$				$R_s = 1\times10^5$			
$\frac{y}{\delta}$	$\frac{l}{\delta}$	$\frac{u}{v_*}$	$\frac{u}{u_e}$	$\frac{y}{\delta}$	$\frac{l}{\delta}$	$\frac{u}{v_*}$	$\frac{u}{u_e}$
0		0	0	0		0	0
				.00005	0	5.00	.1415
.0001	0	5.00	.1489	.0001	.00002000	8.22	.2327
.0003	.00007998	9.64	.2870	.0002	.00005999	10.60	.3000
.0005	.0001599	11.22	.3343	.0006	.0002198	13.75	.3894
.001	.0003595	13.17	.3923	.001	.0003794	15.10	.4275
.002	.0007578	15.01	.4471	.002	.0007776	16.89	.4781
.006	.002338	17.87	.5323	.006	.002358	19.71	.5581
.01	.003900	19.18	.5712	.01	.003919	21.01	.5949
.02	.007717	20.96	.6243	.02	.007735	22.79	.6453
.06	.02180	23.90	.7119	.06	.02181	25.73	.7284
.1	.03405	25.34	.7546	.1	.03407	27.17	.7691
.2	.05742	27.47	.8181	.2	.05743	29.30	.8294
.4	.07871	30.01	.8936	.4	.07872	31.75	.8989
.6	.07728	31.78	.9465	.6	.07728	33.53	.9491
.8	.06656	33.06	.9845	.8	.06656	34.80	.9852
1	.06000	33.58	1	1	.06000	35.32	1

$R_s = 2\times10^5$				$R_s = 5\times10^5$			
$\frac{y}{\delta}$	$\frac{l}{\delta}$	$\frac{u}{v_*}$	$\frac{u}{u_e}$	$\frac{y}{\delta}$	$\frac{l}{\delta}$	$\frac{u}{v_*}$	$\frac{u}{u_e}$
0		0	0	0		0	0
				.00001	0	5.00	.1278
.000025	0	5.00	.1343	.00003	.00000800	9.31	.2380
.00005	.00001000	8.22	.2207	.00005	.00001600	10.89	.2785
.00015	.00004999	11.88	.3190	.00015	.00005599	13.97	.3571
.0005	.0001899	15.20	.4081	.0005	.0001959	17.12	.4378
.001	.0003894	16.99	.4561	.001	.0003954	18.88	.4828
.002	.0007876	18.75	.5035	.002	.0007935	20.63	.5275
.006	.002368	21.56	.5789	.006	.002374	23.43	.5991
.01	.003929	22.86	.6137	.01	.003934	24.72	.6322
.02	.007745	24.63	.6614	.02	.007750	26.50	.6776
.06	.02182	27.57	.7403	.06	.02183	29.43	.7526
.1	.03407	29.00	.7788	.1	.03408	30.87	.7893
.2	.05744	31.14	.8360	.2	.05744	33.00	.8438
.4	.07872	33.67	.9041	.4	.07872	35.54	.9087
.6	.07728	35.45	.9518	.6	.07728	37.31	.9541
.8	.06656	36.72	.9860	.8	.06656	38.59	.9867
1	.06000	37.24	1	1	.06000	39.11	1